

Design of Isolated Bridges from the Viewpoint of Collapse under Extreme Earthquakes



D.W. Chang, Y.T. Lin, C.H. Peng, C.Y. Liou

CECI Engineering Consultants, Inc., Taiwan

T.Y. Lee

National Central University, Taiwan

SUMMARY

This paper is aimed to study the design of isolated bridges based on the ultimate behaviour under extreme earthquakes. Recently, modern bridge seismic design has been developed toward the seismic performance design on whole bridges as well as their components. Understanding of the performance of the components of bridges under extreme earthquakes shall be favourable to design isolated bridges to minimize the damage. Since the Vector Form Intrinsic Finite Element is superior in managing highly nonlinear engineering problems even with fracture and collapse, it is used in this study to predict the failure process of bridges under strong earthquakes. A parametric study on the isolators for a six-span isolated bridge is conducted. The simulation results show that the bridge with the isolators of smaller fracture shear strain performs better in the ultimate state. An optimum design of the stiffness of isolators can be found to minimize the seismic damage.

Keywords: Isolated bridge, Bridge design, Seismic response, Collapse mechanism, Near-field ground motion

1. INTRODUCTION

Isolation technology is a superior countermeasure to mitigate the induced seismic forces for infrastructure especially in earthquake-prone areas. Isolators are generally installed on the top of columns to separate the bridge superstructures from the substructures thereof. Through the elongation of structural vibration period, the induced seismic forces decrease so that bridges can undergo strong earthquakes without severe damage as compared to traditional bridges. However, because the displacements of the superstructures of isolated bridges become excessively large, pounding may occur between adjacent superstructures. The pounding may result in damage on bridges, such as crush of reinforced-concrete slabs, deck unseating. In addition, the past studies reveal that the columns of isolated bridges may exhibit highly nonlinear behaviour under extreme ground motions. Recently, modern bridge seismic design has been developed toward the seismic performance design on whole bridges as well as their components. Understanding of the performance of the components of isolated bridges, such as superstructures, isolators, columns, under extreme earthquakes shall be favourable to design the isolated bridges to minimize the damage.

The Vector Form Intrinsic Finite Element (VFIFE), a new computational method developed by Ting et al., is adopted in this study to simulate the failure process of isolated bridges. A practical isolated bridge with a six-span deck is analyzed under extreme near-field ground motions to predict the collapse mechanism while considering pounding effect of superstructures. High-damping-rubber isolators are installed between the superstructures and the columns or the abutments. A study of isolator design parameters is conducted to realize the interactive responses among the superstructures, isolators and columns. Finally, an optimum design concept for isolated bridges is suggested based on the simulation results of the failure sequence of the structural components and the ultimate collapse of the whole bridge.

2. VECTOR FORM INTRINSIC FINITE ELEMENT

The Vector Form Intrinsic Finite Element (VFIFE) is developed based on theory of physics to mainly simulate failure responses of structural systems subjected to extreme loads. To analyze a continuous structural system by using the VFIFE, a lumped-mass idealization is first performed to construct a discrete model. All lumped masses are then connected by deformable elements without mass which exhibit resisting forces during deformation. Applying Newton's Second Law of Motion, the equations of motion are assembled at each mass for all degrees of freedoms. Assume that a structural system consists of a finite number of particles. The equations of motion for a particle α are written as

$$\mathbf{M}^\alpha \ddot{\mathbf{d}}^\alpha(t) = \mathbf{P}^\alpha(t) - \mathbf{f}^\alpha(t) \quad (2.1)$$

where \mathbf{M}^α is the diagonal mass matrix of the particle α and $\mathbf{d}^\alpha(t)$ is the displacement vector when the particle α is at time t ; \mathbf{P}^α is the vector of applied forces or equivalent forces acting on the particle; \mathbf{f}^α is the vector of the total resistance forces or internal resultant forces exerted by all the elements connecting with this particle.

It is noted that each element without mass is assumed to be in static equilibrium. Observed from Eq. (2.1), the VFIFE analysis is exempted from the assemblage of the global stiffness matrix for structures consisting of elements with multiple degrees of freedom. Therefore, a matrix algebraic operation for the entire system is not required. In stead, each equation of motion for each particle, Eq. (2.1), can be individually solved. Since the failure of structures involves changes in material properties and structural configuration, it is necessary to use discrete time domain analysis to solve the equations of motion. The central difference method, an explicit time integration method, is thus selected in the VFIFE to solve the equations of motion, Eq. (2.1).

Compared to the traditional finite element method, the unique of the VFIFE is that element internal forces are calculated by using the element deformations obtained through subtracting rigid body displacements from total displacements. A set of deformation coordinates is defined for each element in each time increment to calculate the element deformations. Therefore, the VFIFE is capable of dealing with structural dynamic problems with large displacements, deformations and rigid body motion simultaneously.

3. SIMULATION OF ULTIMATE STATES

When subjected to extreme earthquakes, bridges may undergo highly nonlinear behaviour even structural failure. In the past large earthquakes, some bridges suffered deck unseating. Generally, deck unseating follows high material nonlinearity, geometric nonlinearity as well as rigid body motion. To simulate the ultimate states of bridges, the failure mechanism of major bridge components should be taken into account.

The studied failure components are isolators, unseating prevention devices and plastic hinges of decks and columns. Firstly, isolators are idealized as a bilinear model. Once the resistance force of an isolator reaches the designated rupture strength, the isolator fractures and then no longer exerts resistance shear force. Assume that the isolator becomes a sliding-like bearing and friction force exists on the fractured surface. When the relative displacement between superstructure and column exceeds the unseating prevention length, the superstructure will lose the supporting force provided by the column and then fall down from the cap beam due to the gravity force. The failure of isolators represents a typical failure mechanism completing material linear behaviour, material nonlinear behaviour, fracture, and sliding of structures. Such elements in the VFIFE have been developed in the previous studies. This paper herein introduces the element with a gap or a hook, the analytical methods for sliding structures and fracture of elements in the VFIFE (Lee et al. 2009, 2010).

3.1. Gap/Hook Elements

To simulate the pounding effect, the pounding force during collision is modelled by impact elements. A linear elastic spring model is first developed by Kawashima and Penzien (1979). This impact model consisting of an elastic spring and a gap is simple and extensively used element.

The unseating prevention devices are with non-working length before they are triggered to function. There are two categories of the unseating prevention devices, compression and tension. The compression device, such as a stopper, is idealized as an element with a gap, whereas the tension device is idealized as an element with a hook. The elements with a gap or a hook in the VIFIFE have been developed for studying the effectiveness of unseating prevention devices. (Lee et al., 2009, 2010).

3.2. Sliding Elements

After an isolator ruptures, the interface between the superstructure and the column turns to a sliding surface if the relative displacement between the superstructure and the column is still within the unseating prevention length. The motion on the sliding surface can be separated into stick and slip phases. When the friction force is smaller than the maximum static friction force, there is no relative motion in the interface, namely in stick phase. Once the friction force overcomes the maximum static friction force, relative movement starts in the interface and the friction force converts to dynamic friction force, namely in slip phase. In this study, assume that the maximum static friction force is equal to the dynamic friction force, and the dynamic friction coefficient remains constant during sliding.

In the calculation process of the VFIFE, the material properties and structural configuration are assumed to be unchangeable in each time increment. Therefore, the interface should be in either stick phase or slip phase during each incremental time. Before solving the response at the next time step $i+1$, the condition at the interface must be determined. In this study shear-balance procedure, which was proposed by Wang et al. (2001) for analyzing sliding structures by state-space approach, is used to determine the phase of the interface.

On assumption of stick phase, the friction force on the interface is first calculated. It is noted that the relative displacement is null in stick phase. If the calculated friction force is less than the dynamic friction force, the interface is in stick phase. Inversely, if the calculated friction force is equal or larger than the dynamic friction force, it is in slip phase. Figure 1 illustrates the motion of the superstructure with mass M^p and the column with M^b at time step i and $i+1$. The equations of motion for the two masses in the central difference equations are as follows:

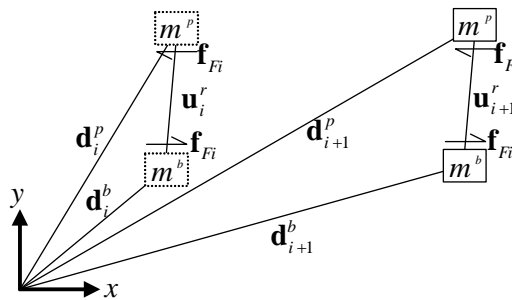


Figure 1. The motion of the superstructure and the column

$$\hat{\mathbf{K}}^p \mathbf{d}_{i+1}^p = \hat{\mathbf{P}}_i^p - \mathbf{f}_{Fi} \quad (3.1)$$

$$\hat{\mathbf{K}}^b \mathbf{d}_{i+1}^b = \hat{\mathbf{P}}_i^b + \mathbf{f}_{Fi} \quad (3.2)$$

where $\hat{\mathbf{K}}^p$, $\hat{\mathbf{P}}_i^p$ are the effective stiffness and force, respectively; \mathbf{f}_{Fi} is the friction force on the interface. If the interface is in stick phase, the relative displacement $\mathbf{u}_i = \mathbf{d}_i^p - \mathbf{d}_i^b$ between the superstructure and the column at time step i is the same as the relative displacement $\mathbf{u}_{i+1} = \mathbf{d}_{i+1}^p - \mathbf{d}_{i+1}^b$ at time step $i+1$.

$$\mathbf{d}_{i+1}^p - \mathbf{d}_{i+1}^b = \mathbf{d}_i^p - \mathbf{d}_i^b \quad (3.3)$$

Rearranging and substituting Eqs. (3.1) and (3.2) into Eq. (3.3), the calculated friction force $\tilde{\mathbf{f}}_{Fi}$ is obtained as

$$\tilde{\mathbf{f}}_{Fi} = \frac{\hat{\mathbf{K}}^b \hat{\mathbf{P}}_i^p - \hat{\mathbf{K}}^p \hat{\mathbf{P}}_i^b - \hat{\mathbf{K}}^p \hat{\mathbf{K}}^b (\mathbf{u}_i^p - \mathbf{u}_i^b)}{\hat{\mathbf{K}}^p + \hat{\mathbf{K}}^b} \quad (3.4)$$

If the calculated friction force $\tilde{\mathbf{f}}_{Fi}$ is less than the dynamic friction force, the assumption of stick phase is true and the calculated friction force can be used in the next time increment, namely $\mathbf{f}_{Fi} = \tilde{\mathbf{f}}_{Fi}$. Otherwise, the interface is in slip phase. The friction force \mathbf{f}_{Fi} must be substituted by dynamic friction force μN , namely $\mathbf{f}_{Fi} = \mu N$. The above can be summarized as

$$\begin{cases} \mathbf{f}_{Fi} = \mu N & \text{if } \tilde{\mathbf{f}}_{Fi} \geq \mu N, \text{ slip phase} \\ \mathbf{f}_{Fi} = \tilde{\mathbf{f}}_{Fi} & \text{if } \tilde{\mathbf{f}}_{Fi} < \mu N, \text{ stick phase} \end{cases} \quad (3.5)$$

3.3. Fracture of Elements

The bilinear model is also used to idealize reinforced concrete columns and steel columns. No matter how the elements may change properties and configuration, even fracture in each time step, they are assumed to be unchangeable in each time interval $t_i \leq t \leq t_{i+1}$ in the VFIFE. Thus, the internal forces are calculated based on the element properties and configuration at the initial time t_i . The deformation coordinates of elements are redefined at the beginning of each time step. In other words, once an element undergoes nonlinear or discontinuous behaviour, all changes are reflected only at the beginning of next time step.

4. TARGET BRIDGE

An isolated bridge based on Japan highway design codes is analyzed under extreme near-field ground motions to predict the collapse mechanism while considering pounding effect of superstructures. High-damping-rubber isolators are installed between the superstructures and the columns or the abutments. This bridge consists of a six-span deck with a total length of $6 \times 40 \text{ m} = 240 \text{ m}$ and a width of 12 m , which is supported by five reinforced concrete columns with a height of 12 m in each and two abutments, as shown in Figure 2. The columns are idealized as a perfect elastoplastic model with a fracture ductility of 21.5 shown in Figure 3(a). The isolators are idealized as a bilinear elastoplastic model shown in Figure 3(b). The initial stiffness and fracture shear strain are the parameters studied. After isolators rupture, the dynamic friction coefficient on the fracture interface is assumed to be 0.15.

The pounding effect of two adjacent decks is also considered by using an element with a gap of 28 cm . The unseating prevention length at each column and abutment is 96 cm . In simulation, the bridges are subjected to near-field ground motions recorded at JR Takatori station, in the 1995 Kobe, Japan earthquake, as shown in Figure 4. The ground acceleration is amplified from 100% to 300% at an

increment of 10%.

5. NUMERICAL SIMULATIONS

A parametric study of the isolator properties is conducted to realize the ultimate dynamic behaviour of the whole bridge. The studied parameters are the initial stiffness and fracture shear strain. Although the fracture shear strain is an inherent or nominal property of isolators, the actual fracture shear strain under extreme earthquakes is mostly different from the designated one. In this research, the fracture shear strain is assumed to be 200%, 300%, 400% and 500%. Additionally, the initial shear stiffness in original design is 2302 MN/m. It is modified to 70%, 85%, 115% and 130 % of the original one in the cases with different fracture shear strain.

Through numerical simulations in cases with various parameters of isolators, the ultimate states are demonstrated and compared. Figures 5 and 6 depict the failure procedure of the target bridge in the cases with the same initial shear stiffness but with different fracture shear strain of 300% and 500%, respectively, under 260% of the JR Takatori record. The first characters C, D, R of the notions in the figures denote the column, deck and isolator, respectively. With comparison between two cases, most of the isolators in the case with fracture shear strain of 300% fail earlier than the plastic hinges of the columns reach the fracture ductility of 21.5. However, all the columns fail earlier than the isolators on them in the case with fracture shear strain of 500%. It is noted that deck unseating is totally attributed to the column falling.

Figures 7 and 8 compare the failure process and ultimate condition in the two cases with 135% and 85 % of the initial shear stiffness. Obviously, the bridge in the case with 85 % of the initial shear stiffness suffers little damage. Only two decks unseat due to the failure of the column C2. In the case with 135% of the initial shear stiffness, all the columns fail earlier than the isolators on them so that all decks unseat due to loss of support.

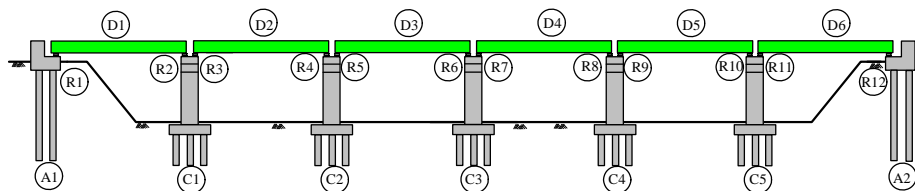


Figure 2. A six-span isolated bridge

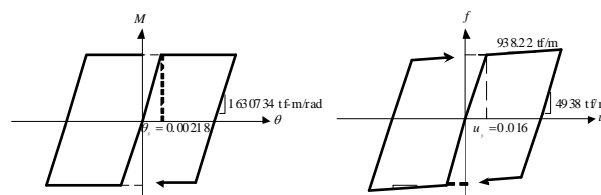


Figure 3. Material property (a) column (b) isolator

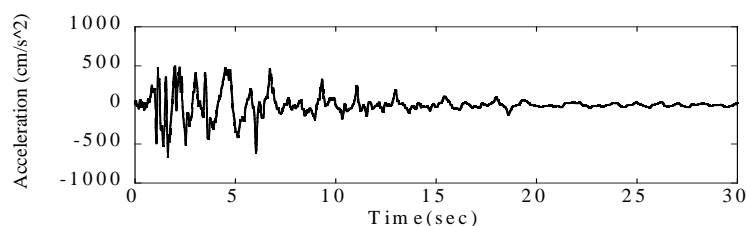


Figure 4. Ground motion recorded at JR-Takatori station in the 1995 Kobe earthquake

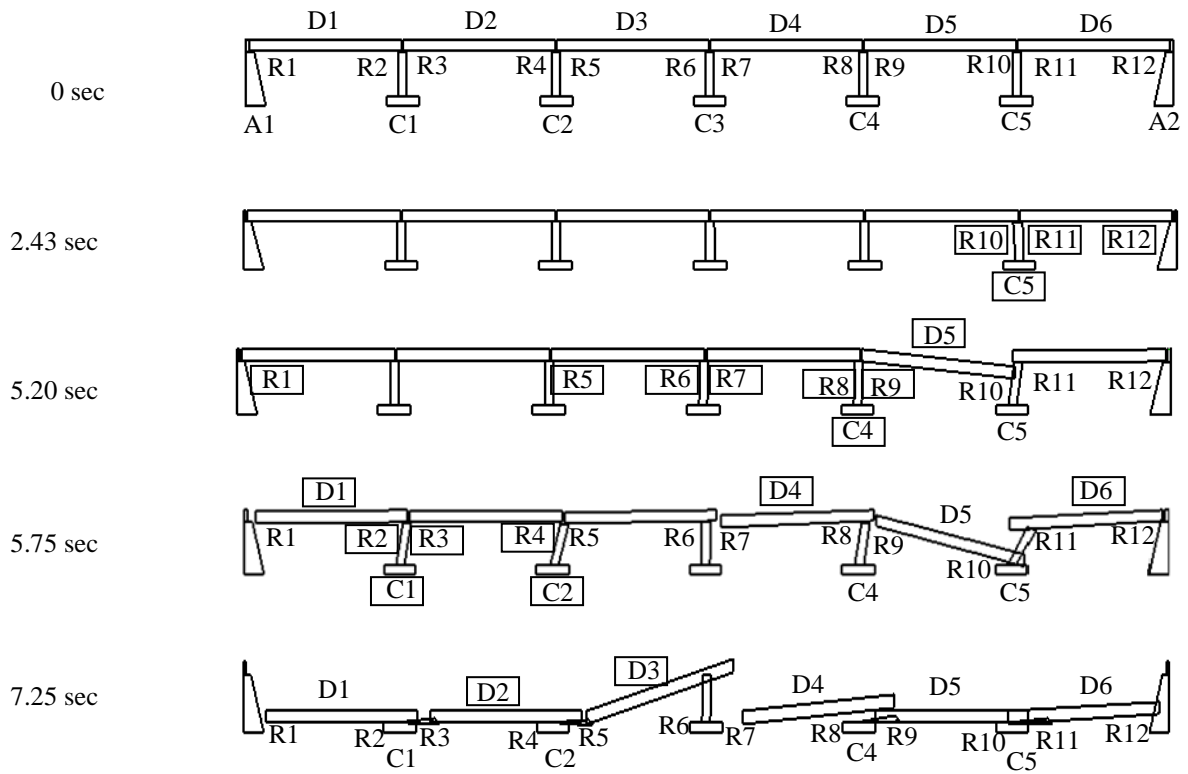


Figure 5. Failure process of the target bridge with the fracture shear strain of 300% under 260% of the JR Takatori record.

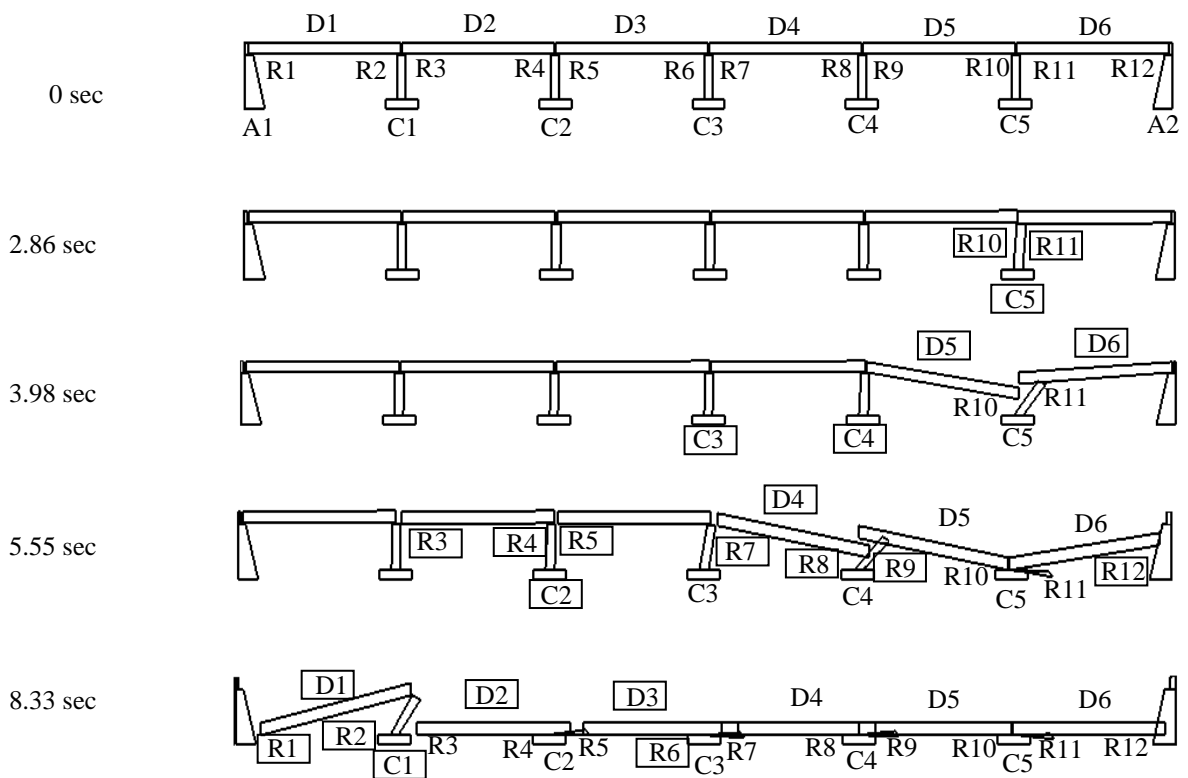


Figure 6. Failure process of the target bridge with the fracture shear strain of 500% under 260% of the JR Takatori record.

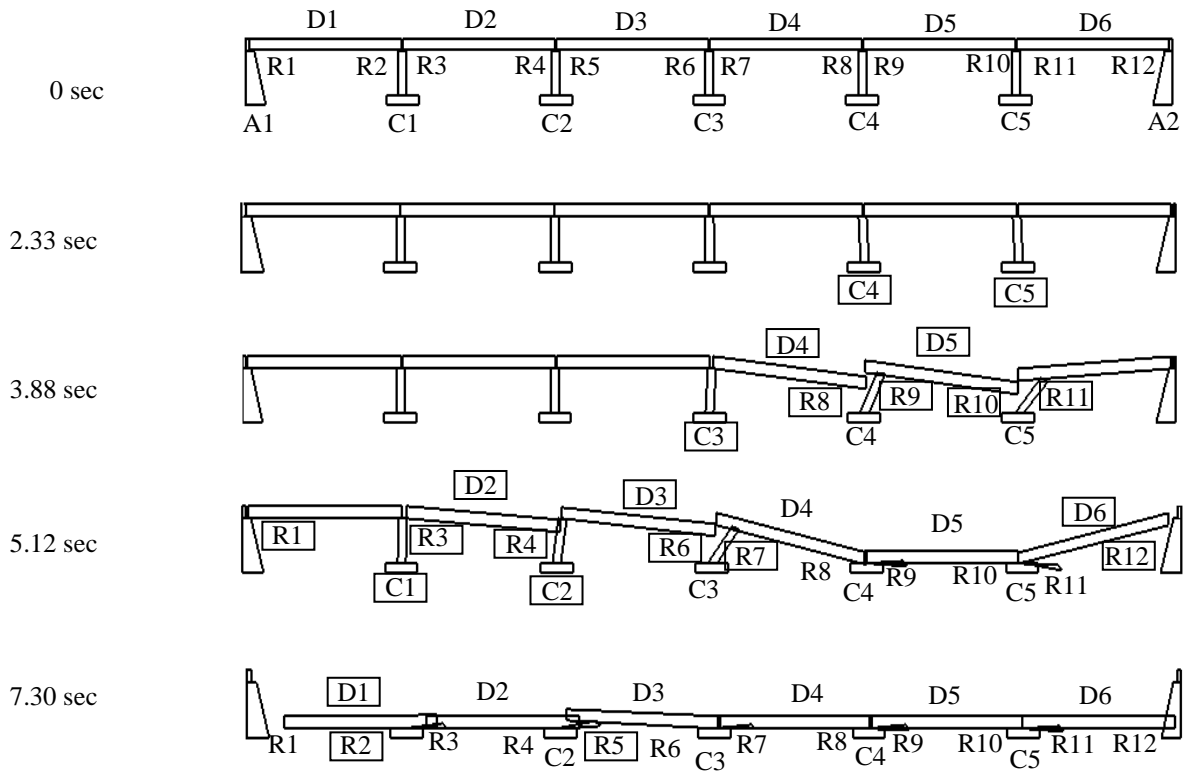


Figure 7. Failure process of the target bridge with the fracture shear strain of 500% and 130% of the original shear stiffness under 260% of the JR Takatori record.

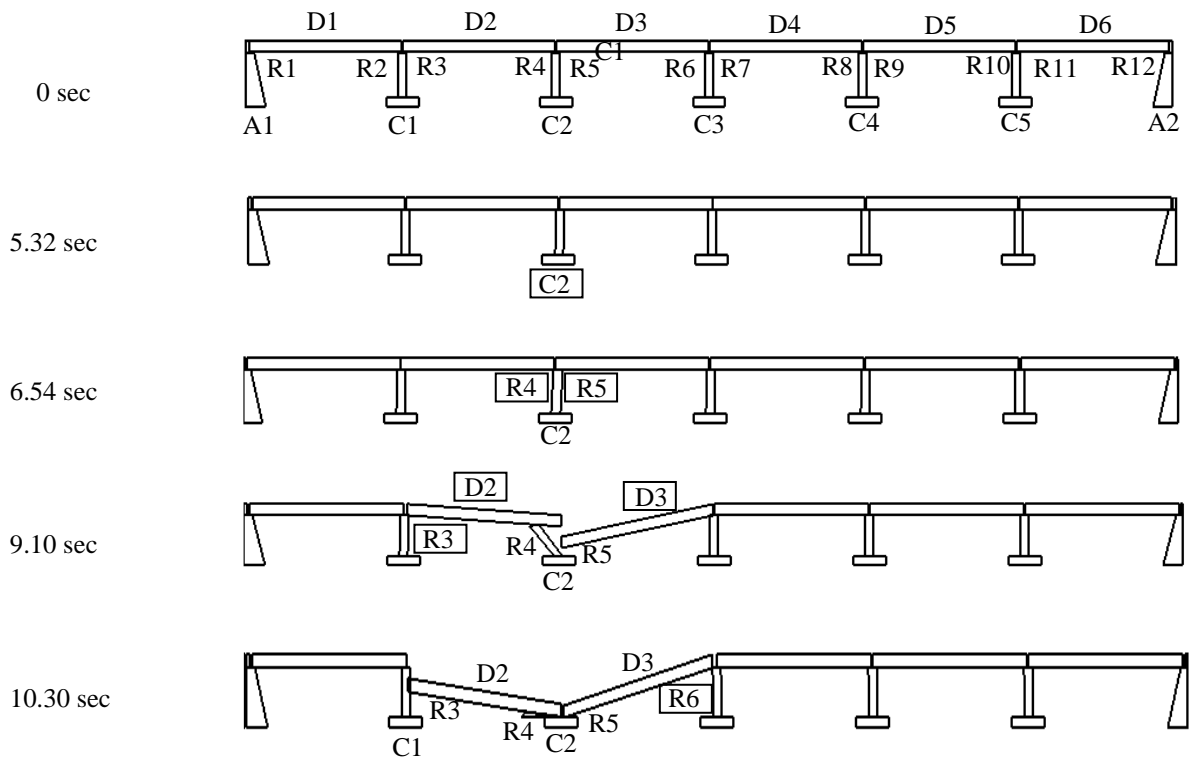


Figure 8. Failure process of the target bridge with the fracture shear strain of 500% and 85% of the original shear stiffness under 260% of the JR Takatori record.

As observed from the cases with different fracture shear strain of isolators, deck unseating never occurs in the case with the fracture shear strain of 200% when the bridge is subjected to the ground motion up to 300% of the JR Takatori record. In the other cases with larger fracture shear strain, deck unseating occurs under the ground motion being equal to and larger than 240% of the JR Takatori record. However, the collapse mechanism of the whole bridge is varying as the fracture shear strain increases. In the case with smaller fracture shear strain the isolators rupture first and then the induced seismic force is not transmitted any longer to the substructures. Since the isolators behave like sliding bearings, the decks unseat is due to the insufficient unseating length. Inversely, in the case with larger fracture shear strain the plastic hinge at the bottom of columns occurs earlier. Once the ductility of the plastic hinge reaches the fracture ductility of 21.5, the column cannot carry moment force any longer so that the bridge collapses due to column failure.

For the cases with different initial stiffness of isolators, the structural vibration periods decrease as the initial stiffness of isolators increases, and vice versa. The simulation results show that in the cases with larger initial stiffness of isolators the bridge suffers deck unseating under smaller ground motion. It is noted that in the case with 85% of the original shear stiffness the deck unseating occurs under the largest ground motion as compared to the other cases.

6. CONCLUSIONS

This research is aimed to study the design of isolated bridges based on the ultimate dynamic behaviour under extreme earthquakes. Since the VFIFE is superior in managing the engineering problems with material nonlinearity, discontinuity, large deformation, large displacement, arbitrary rigid body motions of deformable bodies and even fracture and collapse, it is used in this study to predict the failure process of the bridges under strong earthquakes. A six-span isolated bridge with high-damping-rubber isolators is analyzed under the JR Takatori ground motion amplified from 100% to 300%. A parametric study on the high-damping-rubber isolators is performed to realize the ultimate state of the bridge. The simulation results show that the bridge with the isolators of larger fracture shear strain suffer severer damage because larger seismic induced force is transmitted to the substructures. The columns fail earlier than the isolators on them. When the fracture shear strain is small enough, namely 200%, the target bridge does not suffer deck unseating even though the JR Takatori ground motion is amplified to 300%. In addition, when the initial stiffness of the isolators is regulated, the simulation results reveal that the bridge with higher initial shear stiffness of isolators suffers more unseating decks. However, the bridge with the isolators of 85% of the original shear stiffness behaves superior than that in the other cases. There is optimum isolator stiffness in the target bridge to minimize the damage under extreme earthquakes.

REFERENCES

- Kawashima, K. and Penzien, J. (1979). Theoretical and experimental dynamic behavior of a curved model bridge structure. *Earthquake Engineering and Structural Dynamics* **7:2**, 129-145.
- Kalkan, E. and Kunnath, S. K. (2006). Effects of Fling Step and Forward Directivity on Seismic Response of Buildings. *Earthquake Spectra*. **22:2**, 367-390.
- Lee, T.Y., Chen, P.H. and Wang, R.Z. (2009). Dynamic analysis of bridges in the ultimate state under earthquakes. *Sixth International Conference on Urban Earthquake Engineering*, Tokyo, Japan, March 3-4.
- Lee, T.Y., Wong, P.L. and Wang, R.Z. (2010). Dynamic behavior of seismic-excited bridges in ultimate states. *Proc. of 9th U.S. National and 10th Canadian Conference on Earthquake Engineering*. Toronto, Canada, July 25-29.
- Lee, T.-Y., Chen, K.T. and Su, C.C. (2011). Pounding effects on bridges during extreme earthquakes. *Proc. of 8th International Conference on Structural Dynamics*. Leuven, Belgium, July 4-6.
- Ruangrassamee, A. and Kawashima, K. (2003). Control of nonlinear bridge response with pounding effect by variable dampers. *Engineering Structures*. **25:5**, 596-606.
- Ting, E. C., Shih, C. and Wang Y. K. (2004). Fundamentals of a vector form intrinsic finite element: Part I. basic procedure and a plane frame element. *Journal of Mechanics*. **20:2**, 113-122.

- Tirasit, P. and Kawashima, K. 2008. Effect of nonlinear seismic torsion on the performance of skewed bridge piers. *Journal of Earthquake Engineering*. **12:6**, 980-998.
- Wang Y.P., Liao W. H. and Lee, C.L. (2001). A state-space approach for dynamic analysis of sliding structures. *Engineering Structures*, **23:7**, 790-801.